

**Bose-Einstein Correlations of Charged Pion Pairs  
in Au+Au Collisions at  $\sqrt{s_{NN}} = 200$  GeV.**

S.S. Adler,<sup>5</sup> S. Afanasiev,<sup>17</sup> C. Aidala,<sup>5</sup> N.N. Ajitanand,<sup>43</sup> Y. Akiba,<sup>20,38</sup> J. Alexander,<sup>43</sup> R. Amirkas,<sup>12</sup> L. Aphecetche,<sup>45</sup> S.H. Aronson,<sup>5</sup> R. Auerbeck,<sup>44</sup> T.C. Awes,<sup>35</sup> R. Azmoun,<sup>44</sup> V. Babintsev,<sup>15</sup> A. Baldisseri,<sup>10</sup> K.N. Barish,<sup>6</sup> P.D. Barnes,<sup>27</sup> B. Bassalleck,<sup>33</sup> S. Bathe,<sup>30</sup> S. Batsouli,<sup>9</sup> V. Baublis,<sup>37</sup> A. Bazilevsky,<sup>39,15</sup> S. Belikov,<sup>16,15</sup> Y. Berdnikov,<sup>40</sup> S. Bhagavatula,<sup>16</sup> J.G. Boissevain,<sup>27</sup> H. Borel,<sup>10</sup> S. Borenstein,<sup>25</sup> M.L. Brooks,<sup>27</sup> D.S. Brown,<sup>34</sup> N. Bruner,<sup>33</sup> D. Bucher,<sup>30</sup> H. Buesching,<sup>30</sup> V. Bumazhnov,<sup>15</sup> G. Bunce,<sup>5,39</sup> J.M. Burward-Hoy,<sup>26,44</sup> S. Butsyk,<sup>44</sup> X. Camard,<sup>45</sup> J.-S. Chai,<sup>18</sup> P. Chand,<sup>4</sup> W.C. Chang,<sup>2</sup> S. Chernichenko,<sup>15</sup> C.Y. Chi,<sup>9</sup> J. Chiba,<sup>20</sup> M. Chiu,<sup>9</sup> I.J. Choi,<sup>52</sup> J. Choi,<sup>19</sup> R.K. Choudhury,<sup>4</sup> T. Chujo,<sup>5</sup> V. Cianciolo,<sup>35</sup> Y. Cobigo,<sup>10</sup> B.A. Cole,<sup>9</sup> P. Constantin,<sup>16</sup> D.G. d'Enterria,<sup>45</sup> G. David,<sup>5</sup> H. Delagrange,<sup>45</sup> A. Denisov,<sup>15</sup> A. Deshpande,<sup>39</sup> E.J. Desmond,<sup>5</sup> O. Dietzsch,<sup>41</sup> O. Drapier,<sup>25</sup> A. Drees,<sup>44</sup> R. du Rietz,<sup>29</sup> A. Durum,<sup>15</sup> D. Dutta,<sup>4</sup> Y.V. Efremenko,<sup>35</sup> K. El Chenawi,<sup>49</sup> A. Enokizono,<sup>14</sup> H. En'yo,<sup>38,39</sup> S. Esumi,<sup>48</sup> L. Ewell,<sup>5</sup> D.E. Fields,<sup>33,39</sup> F. Fleuret,<sup>25</sup> S.L. Fokin,<sup>23</sup> B.D. Fox,<sup>39</sup> Z. Fraenkel,<sup>51</sup> J.E. Frantz,<sup>9</sup> A. Franz,<sup>5</sup> A.D. Frawley,<sup>12</sup> S.-Y. Fung,<sup>6</sup> S. Garpman,<sup>29</sup> \* T.K. Ghosh,<sup>49</sup> A. Glenn,<sup>46</sup> G. Gogiberidze,<sup>46</sup> M. Gonin,<sup>25</sup> J. Gosset,<sup>10</sup> Y. Goto,<sup>39</sup> R. Granier de Cassagnac,<sup>25</sup> N. Grau,<sup>16</sup> S.V. Greene,<sup>49</sup> M. Grosse Perdekamp,<sup>39</sup> W. Guryn,<sup>5</sup> H.-Å. Gustafsson,<sup>29</sup> T. Hachiya,<sup>14</sup> J.S. Haggerty,<sup>5</sup> H. Hamagaki,<sup>8</sup> A.G. Hansen,<sup>27</sup> E.P. Hartouni,<sup>26</sup> M. Harvey,<sup>5</sup> R. Hayano,<sup>8</sup> X. He,<sup>13</sup> M. Heffner,<sup>26</sup> T.K. Hemmick,<sup>44</sup> J.M. Heuser,<sup>44</sup> M. Hibino,<sup>50</sup> J.C. Hill,<sup>16</sup> W. Holzmann,<sup>43</sup> K. Homma,<sup>14</sup> B. Hong,<sup>22</sup> A. Hoover,<sup>34</sup> T. Ichihara,<sup>38,39</sup> V.V. Ikonnikov,<sup>23</sup> K. Imai,<sup>24,38</sup> D. Isenhower,<sup>1</sup> M. Ishihara,<sup>38</sup> M. Issah,<sup>43</sup> A. Isupov,<sup>17</sup> B.V. Jacak,<sup>44</sup> W.Y. Jang,<sup>22</sup> Y. Jeong,<sup>19</sup> J. Jia,<sup>44</sup> O. Jinnouchi,<sup>38</sup> B.M. Johnson,<sup>5</sup> S.C. Johnson,<sup>26</sup> K.S. Joo,<sup>31</sup> D. Jouan,<sup>36</sup> S. Kametani,<sup>8,50</sup> N. Kamihara,<sup>47,38</sup> J.H. Kang,<sup>52</sup> S.S. Kapoor,<sup>4</sup> K. Katou,<sup>50</sup> S. Kelly,<sup>9</sup> B. Khachaturov,<sup>51</sup> A. Khanzadeev,<sup>37</sup> J. Kikuchi,<sup>50</sup> D.H. Kim,<sup>31</sup> D.J. Kim,<sup>52</sup> D.W. Kim,<sup>19</sup> E. Kim,<sup>42</sup> G.-B. Kim,<sup>25</sup> H.J. Kim,<sup>52</sup> E. Kistenev,<sup>5</sup> A. Kiyomichi,<sup>48</sup> K. Kiyoyama,<sup>32</sup> C. Klein-Boesing,<sup>30</sup> H. Kobayashi,<sup>38,39</sup> L. Kochenda,<sup>37</sup> V. Kochetkov,<sup>15</sup> D. Koehler,<sup>33</sup> T. Kohama,<sup>14</sup> M. Kopytine,<sup>44</sup> D. Kotchetkov,<sup>6</sup> A. Kozlov,<sup>51</sup> P.J. Kroon,<sup>5</sup> C.H. Kuberg,<sup>1,27</sup> K. Kurita,<sup>39</sup> Y. Kuroki,<sup>48</sup> M.J. Kweon,<sup>22</sup> Y. Kwon,<sup>52</sup> G.S. Kyle,<sup>34</sup> R. Lacey,<sup>43</sup> V. Ladygin,<sup>17</sup> J.G. Lajoie,<sup>16</sup> A. Lebedev,<sup>16,23</sup> S. Leckey,<sup>44</sup> D.M. Lee,<sup>27</sup> S. Lee,<sup>19</sup> M.J. Leitch,<sup>27</sup> X.H. Li,<sup>6</sup> H. Lim,<sup>42</sup> A. Litvinenko,<sup>17</sup> M.X. Liu,<sup>27</sup> Y. Liu,<sup>36</sup> C.F. Maguire,<sup>49</sup> Y.I. Makdisi,<sup>5</sup> A. Malakhov,<sup>17</sup> V.I. Manko,<sup>23</sup> Y. Mao,<sup>7,38</sup> G. Martinez,<sup>45</sup> M.D. Marx,<sup>44</sup> H. Masui,<sup>48</sup> F. Matathias,<sup>44</sup> T. Matsumoto,<sup>8,50</sup> P.L. McGaughey,<sup>27</sup> E. Melnikov,<sup>15</sup> F. Messer,<sup>44</sup> Y. Miake,<sup>48</sup> J. Milan,<sup>43</sup> T.E. Miller,<sup>49</sup> A. Milov,<sup>44,51</sup> S. Mioduszewski,<sup>5</sup> R.E. Mischke,<sup>27</sup> G.C. Mishra,<sup>13</sup> J.T. Mitchell,<sup>5</sup> A.K. Mohanty,<sup>4</sup> D.P. Morrison,<sup>5</sup> J.M. Moss,<sup>27</sup> F. Mühlbacher,<sup>44</sup> D. Mukhopadhyay,<sup>51</sup> M. Muniruzzaman,<sup>6</sup> J. Murata,<sup>38,39</sup> S. Nagamiya,<sup>20</sup> J.L. Nagle,<sup>9</sup> T. Nakamura,<sup>14</sup> B.K. Nandi,<sup>6</sup> M. Nara,<sup>48</sup> J. Newby,<sup>46</sup> P. Nilsson,<sup>29</sup> A.S. Nyanin,<sup>23</sup> J. Nystrand,<sup>29</sup> E. O'Brien,<sup>5</sup> C.A. Ogilvie,<sup>16</sup> H. Ohnishi,<sup>5,38</sup> I.D. Ojha,<sup>49,3</sup> K. Okada,<sup>38</sup> M. Ono,<sup>48</sup> V. Onuchin,<sup>15</sup> A. Oskarsson,<sup>29</sup> I. Otterlund,<sup>29</sup> K. Oyama,<sup>8</sup> K. Ozawa,<sup>8</sup> D. Pal,<sup>51</sup> A.P.T. Palounek,<sup>27</sup> V.S. Pantuev,<sup>44</sup> V. Papavassiliou,<sup>34</sup> J. Park,<sup>42</sup> A. Parmar,<sup>33</sup> S.F. Pate,<sup>34</sup> T. Peitzmann,<sup>30</sup> J.-C. Peng,<sup>27</sup> V. Peresedov,<sup>17</sup> C. Pinkenburg,<sup>5</sup> R.P. Pisani,<sup>5</sup> F. Plasil,<sup>35</sup> M.L. Purschke,<sup>5</sup> A.K. Purwar,<sup>44</sup> J. Rak,<sup>16</sup> I. Ravinovich,<sup>51</sup> K.F. Read,<sup>35,46</sup> M. Reuter,<sup>44</sup> K. Reygers,<sup>30</sup> V. Riabov,<sup>37,40</sup> Y. Riabov,<sup>37</sup> G. Roche,<sup>28</sup> A. Romana,<sup>25</sup> M. Rosati,<sup>16</sup> P. Rosnet,<sup>28</sup> S.S. Ryu,<sup>52</sup> M.E. Sadler,<sup>1</sup> N. Saito,<sup>38,39</sup> T. Sakaguchi,<sup>8,50</sup> M. Sakai,<sup>32</sup> S. Sakai,<sup>48</sup> V. Samsonov,<sup>37</sup> L. Sanfratello,<sup>33</sup> R. Santo,<sup>30</sup> H.D. Sato,<sup>24,38</sup> S. Sato,<sup>5,48</sup> S. Sawada,<sup>20</sup> Y. Schutz,<sup>45</sup> V. Semenov,<sup>15</sup> R. Seto,<sup>6</sup> M.R. Shaw,<sup>1,27</sup> T.K. Shea,<sup>5</sup> T.-A. Shibata,<sup>47,38</sup> K. Shigaki,<sup>14,20</sup> T. Shiina,<sup>27</sup> C.L. Silva,<sup>41</sup> D. Silvermyr,<sup>27,29</sup> K.S. Sim,<sup>22</sup> C.P. Singh,<sup>3</sup> V. Singh,<sup>3</sup> M. Sivertz,<sup>5</sup> A. Soldatov,<sup>15</sup> R.A. Soltz,<sup>26</sup> W.E. Sondheim,<sup>27</sup> S.P. Sorensen,<sup>46</sup> I.V. Sourikova,<sup>5</sup> F. Staley,<sup>10</sup> P.W. Stankus,<sup>35</sup> E. Stenlund,<sup>29</sup> M. Stepanov,<sup>34</sup> A. Ster,<sup>21</sup> S.P. Stoll,<sup>5</sup> T. Sugitate,<sup>14</sup> J.P. Sullivan,<sup>27</sup> E.M. Takagui,<sup>41</sup> A. Taketani,<sup>38,39</sup> M. Tamai,<sup>50</sup> K.H. Tanaka,<sup>20</sup> Y. Tanaka,<sup>32</sup> K. Tanida,<sup>38</sup> M.J. Tannenbaum,<sup>5</sup> P. Tarján,<sup>11</sup> J.D. Tepe,<sup>1,27</sup> T.L. Thomas,<sup>33</sup> J. Tojo,<sup>24,38</sup> H. Torii,<sup>24,38</sup> R.S. Towell,<sup>1</sup> I. Tseruya,<sup>51</sup> H. Tsuruoka,<sup>48</sup> S.K. Tuli,<sup>3</sup> H. Tydesjö,<sup>29</sup> N. Tyurin,<sup>15</sup> H.W. van Hecke,<sup>27</sup> J. Velkovska,<sup>5,44</sup> M. Velkovsky,<sup>44</sup> L. Villatte,<sup>46</sup> A.A. Vinogradov,<sup>23</sup> M.A. Volkov,<sup>23</sup> E. Vznuzdaev,<sup>37</sup> X.R. Wang,<sup>13</sup> Y. Watanabe,<sup>38,39</sup> S.N. White,<sup>5</sup> F.K. Wohn,<sup>16</sup> C.L. Woody,<sup>5</sup> W. Xie,<sup>6</sup> Y. Yang,<sup>7</sup> A. Yanovich,<sup>15</sup> S. Yokkaichi,<sup>38,39</sup> G.R. Young,<sup>35</sup> I.E. Yushmanov,<sup>23</sup> W.A. Zajc,<sup>9,†</sup> C. Zhang,<sup>9</sup> S. Zhou,<sup>7</sup> S.J. Zhou,<sup>51</sup> and L. Zolin<sup>17</sup>

(PHENIX Collaboration)

<sup>1</sup>Abilene Christian University, Abilene, TX 79699, USA

<sup>2</sup>Institute of Physics, Academia Sinica, Taipei 11529, Taiwan

<sup>3</sup>Department of Physics, Banaras Hindu University, Varanasi 221005, India

<sup>4</sup>Bhabha Atomic Research Centre, Bombay 400 085, India

- <sup>5</sup>Brookhaven National Laboratory, Upton, NY 11973-5000, USA  
<sup>6</sup>University of California - Riverside, Riverside, CA 92521, USA  
<sup>7</sup>China Institute of Atomic Energy (CIAE), Beijing, People's Republic of China  
<sup>8</sup>Center for Nuclear Study, Graduate School of Science, University of Tokyo, 7-3-1 Hongo, Bunkyo, Tokyo 113-0033, Japan  
<sup>9</sup>Columbia University, New York, NY 10027 and Nevis Laboratories, Irvington, NY 10533, USA  
<sup>10</sup>Dapnia, CEA Saclay, F-91191, Gif-sur-Yvette, France  
<sup>11</sup>Debrecen University, H-4010 Debrecen, Egyetem tér 1, Hungary  
<sup>12</sup>Florida State University, Tallahassee, FL 32306, USA  
<sup>13</sup>Georgia State University, Atlanta, GA 30303, USA  
<sup>14</sup>Hiroshima University, Kagamiyama, Higashi-Hiroshima 739-8526, Japan  
<sup>15</sup>Institute for High Energy Physics (IHEP), Protvino, Russia  
<sup>16</sup>Iowa State University, Ames, IA 50011, USA  
<sup>17</sup>Joint Institute for Nuclear Research, 141980 Dubna, Moscow Region, Russia  
<sup>18</sup>KAERI, Cyclotron Application Laboratory, Seoul, South Korea  
<sup>19</sup>Kangnung National University, Kangnung 210-702, South Korea  
<sup>20</sup>KEK, High Energy Accelerator Research Organization, Tsukuba-shi, Ibaraki-ken 305-0801, Japan  
<sup>21</sup>KFKI Research Institute for Particle and Nuclear Physics (RMKI), H-1525 Budapest 114, POBox 49, Hungary  
<sup>22</sup>Korea University, Seoul, 136-701, Korea  
<sup>23</sup>Russian Research Center "Kurchatov Institute", Moscow, Russia  
<sup>24</sup>Kyoto University, Kyoto 606, Japan  
<sup>25</sup>Laboratoire Leprince-Ringuet, Ecole Polytechnique, CNRS-IN2P3, Route de Saclay, F-91128, Palaiseau, France  
<sup>26</sup>Lawrence Livermore National Laboratory, Livermore, CA 94550, USA  
<sup>27</sup>Los Alamos National Laboratory, Los Alamos, NM 87545, USA  
<sup>28</sup>LPC, Université Blaise Pascal, CNRS-IN2P3, Clermont-Fd, 63177 Aubiere Cedex, France  
<sup>29</sup>Department of Physics, Lund University, Box 118, SE-221 00 Lund, Sweden  
<sup>30</sup>Institut für Kernphysik, University of Muenster, D-48149 Muenster, Germany  
<sup>31</sup>Myongji University, Yongin, Kyonggido 449-728, Korea  
<sup>32</sup>Nagasaki Institute of Applied Science, Nagasaki-shi, Nagasaki 851-0193, Japan  
<sup>33</sup>University of New Mexico, Albuquerque, NM, USA  
<sup>34</sup>New Mexico State University, Las Cruces, NM 88003, USA  
<sup>35</sup>Oak Ridge National Laboratory, Oak Ridge, TN 37831, USA  
<sup>36</sup>IPN-Orsay, Université Paris Sud, CNRS-IN2P3, BP1, F-91406, Orsay, France  
<sup>37</sup>PNPI, Petersburg Nuclear Physics Institute, Gatchina, Russia  
<sup>38</sup>RIKEN (The Institute of Physical and Chemical Research), Wako, Saitama 351-0198, JAPAN  
<sup>39</sup>RIKEN BNL Research Center, Brookhaven National Laboratory, Upton, NY 11973-5000, USA  
<sup>40</sup>St. Petersburg State Technical University, St. Petersburg, Russia  
<sup>41</sup>Universidade de São Paulo, Instituto de Física, Caixa Postal 66318, São Paulo CEP05315-970, Brazil  
<sup>42</sup>System Electronics Laboratory, Seoul National University, Seoul, South Korea  
<sup>43</sup>Chemistry Department, Stony Brook University, SUNY, Stony Brook, NY 11794-3400, USA  
<sup>44</sup>Department of Physics and Astronomy, Stony Brook University, SUNY, Stony Brook, NY 11794, USA  
<sup>45</sup>SUBATECH (Ecole des Mines de Nantes, CNRS-IN2P3, Université de Nantes) BP 20722 - 44307, Nantes, France  
<sup>46</sup>University of Tennessee, Knoxville, TN 37996, USA  
<sup>47</sup>Department of Physics, Tokyo Institute of Technology, Tokyo, 152-8551, Japan  
<sup>48</sup>Institute of Physics, University of Tsukuba, Tsukuba, Ibaraki 305, Japan  
<sup>49</sup>Vanderbilt University, Nashville, TN 37235, USA  
<sup>50</sup>Waseda University, Advanced Research Institute for Science and Engineering, 17 Kikui-cho, Shinjuku-ku, Tokyo 162-0044, Japan  
<sup>51</sup>Weizmann Institute, Rehovot 76100, Israel  
<sup>52</sup>Yonsei University, IPAP, Seoul 120-749, Korea

(Dated: October 29, 2018)

Bose-Einstein correlations of identically charged pion pairs were measured by the PHENIX experiment at mid-rapidity in Au+Au collisions at  $\sqrt{s_{NN}} = 200$  GeV. The Bertsch-Pratt radius parameters were determined as a function of the transverse momentum of the pair and as a function of the centrality of the collision. Using the *full* Coulomb correction, the ratio  $R_{out}/R_{side}$  is smaller than unity for  $\langle k_T \rangle$  from 0.25 to 1.2 GeV/c and for all measured centralities. However, using recently developed partial Coulomb correction methods, we find that  $R_{out}/R_{side}$  is 0.8-1.1 for the measured  $\langle k_T \rangle$  range, and approximately constant at unity with the number of participants.

PACS numbers: 25.75.Dw

Following its origin in the study of proton-antiproton annihilations [1], Bose-Einstein correlations have been

extensively used to measure source distributions in relativistic heavy ion collisions [2, 3]. These measurements

were originally motivated by theoretical predictions of a large source size and/or a long duration of particle emission [4, 5, 6] – which would result from a softening of the equation-of-state in a first-order phase transition to a quark-gluon plasma (QGP). The technique of Bose-Einstein correlations is based upon quantum statistical interference, but final state interactions such as Coulomb repulsion modify the relative momentum distributions for pairs of identical particles emanating from the collision region. Both effects are included in multidimensional Gaussian fits to the normalized relative momentum distributions yielding the fit parameters which are the RMS-widths in each dimension,  $R_{\text{long}}$ ,  $R_{\text{side}}$ ,  $R_{\text{out}}$  [7, 8], also referred to as HBT radii. A finite duration of emission leads to an effective elongation of one of the HBT radii,  $R_{\text{out}}$ , which is parallel to the mean transverse momentum of pair,  $k_T = (\mathbf{p}_{1T} + \mathbf{p}_{2T})/2$ ; however, the other radii along the axes perpendicular to  $k_T$  represent the geometrical source sizes. Therefore the  $R_{\text{out}}/R_{\text{side}}$  ratio could become larger than unity even for a cylindrical particle source, if a long duration of particle emissions occurs. For dynamic (i.e. expanding) sources, the HBT radii depend on the  $k_T$ , and correspond to lengths of homogeneity, regions of the source which emit particles of similar momentum [9]. Measuring the  $k_T$  dependence of the HBT radii provides essential constraints on dynamical models that include the space-time evolution of the source [10, 11].

Hydrodynamic models for the space-time evolution of a rehadronizing QGP predicted that the measurement of the  $R_{\text{out}}/R_{\text{side}}$  ratio at moderate values of  $k_T$  provides a sensitive test of the long duration of particle emission, a signal of a slowly burning first order phase transition from QGP to hadrons at RHIC [4]. Their predictions that the  $R_{\text{out}}/R_{\text{side}}$  ratio should reach  $\sim 1.5$  at  $k_T$  of  $\sim 0.5$  GeV/c were not borne out by initial measurements of Bose-Einstein correlations of pions from Au+Au collisions at  $\sqrt{s_{\text{NN}}} = 130$  GeV [12, 13]. This disagreement between theory and data has been called the ‘‘RHIC HBT puzzle’’ [14].

We present here data on Bose-Einstein correlations of charged pion pairs measured by the PHENIX experiment at RHIC for Au+Au collisions at  $\sqrt{s_{\text{NN}}} = 200$  GeV. In this analysis, we adopt a recent fitting technique that provides for a self-consistent treatment of the Coulomb final state interaction for a source that is made up of a smaller core and a more extended halo of long-lived resonances. We introduce a new parameterization in which the strength of the Coulomb interaction is constrained by the measured unlike-signed pion correlation.

The PHENIX detector provides particle identification (PID) capabilities for hadrons, leptons and photons over a wide momentum range. The setup of the PHENIX detector has been described in detail elsewhere [15]. In this analysis, we use the west arm of the central spectrometer, which covers the pseudorapidity region  $|\eta| < 0.35$

and  $\Delta\phi = \pi/2$  in azimuthal angle over a region of  $0.2$  GeV/c  $< k_T < 2.0$  GeV/c. The drift chamber (DC), at a radial distance between 2.0 m and 2.4 m, provides trajectory information in the azimuthal direction. A pad chamber (PC1) at 2.5 m provides  $z$ -coordinate information. Combining the DC and PC1 information, a track model provides a 3-dimensional trajectory and momentum vector for charged particles. The momentum resolution is  $\delta p/p \simeq 0.7\% \oplus 1.0\% \times p$  (GeV/c), where the first term is due to the multiple scattering before the DC and the second term is the angular resolution of the DC. For this analysis, the electromagnetic calorimeter (EMCal) provides the time of arrival of particles at its front face located 5.1 m from the beam axis. The timing resolution is approximately 400 psec for hadrons. This analysis is based on a sample of 34 million minimum bias events taken with a magnetic field of 0.78 T·m and triggered by the coincidence of the Beam-Beam Counters (BBC) and Zero-Degree Calorimeters (ZDC) – corresponding to  $92 \pm 2\%$  of the total inelastic cross section of 6.8 b. Event centrality is determined from the correlation between the BBC multiplicity and the analog response of the ZDC. About 23 million events are selected with a requirement that the collision vertex measured by the BBC has  $|z| < 30$  cm. Each track is required to have an associated hit on the EMCal within  $2\sigma$  of the track’s projection to the EMCal, where  $\sigma$  refers to the resolution of the projection. Charged particles are identified by the time-of-flight technique using timing information between the BBC and the EMCal, combined with momentum and flight length calculated by the track model. Charged particles in the PID zone within  $1.5\sigma$  of the ideal squared-mass peak of pions but  $1.5\sigma$  away from the kaon bands are identified as pions. After the track quality and PID cuts,  $\sim 45$  million positive pions and  $\sim 51$  million negative pions are selected in a momentum range from 0.2 to 2.0 GeV/c.

The pion correlation function is experimentally defined as  $C_2(\mathbf{q}) = A(\mathbf{q})/B(\mathbf{q})$ , where  $A(\mathbf{q})$  is the measured two-pion (actual pair) distribution of pair momentum difference  $\mathbf{q}$ , and  $B(\mathbf{q})$  is the background pair (mixed pair) distribution generated using mixed events from the same data sample. Event mixing is done selecting events that have similar multiplicities and event vertices. As in our previous analyses at  $\sqrt{s_{\text{NN}}} = 130$  GeV [12], actual pairs within 1 cm in the beam direction ( $\Delta Z_{DC}$ ) and 0.06 radians in azimuthal angle ( $\Delta\phi_{DC}$ ) in the DC are eliminated from the pair sample to remove ghost tracks, then within 5 cm in  $\Delta Z_{DC}$  and 0.03 radians in  $\Delta\phi_{DC}$  are also eliminated to avoid a strongly inefficient region for pairs. Since pairs which are close to one another in the EMCal are either reconstructed as single hit clusters or are affected by cluster-sharing, pairs whose hits are within 8 cm at the EMCal are eliminated. The background mixed pairs are subject to the same cuts as actual pairs. After the pair cuts,  $\sim 110$  million positive pion pairs and

$\sim 140$  million negative pion pairs remain. The number of pairs is 40 times larger than the data sample used for the PHENIX data at  $\sqrt{s_{NN}} = 130$  GeV [12]. The systematic errors on the HBT radius parameters from the pair cuts are evaluated by varying the pair cuts to be  $\sim 2\%$  for  $R_{\text{side}}$  and  $R_{\text{long}}$ , and  $\sim 7\%$  for  $R_{\text{out}}$ . The correction for the multi-track reconstruction efficiencies in the DC and EMCal are determined by a GEANT-based [16] Monte Carlo (MC) simulation of the detector. The pair efficiencies of the DC and EMCal are estimated by the ratio of the distribution of separations of actual pairs to that of normalized mixed pairs. Also the multiplicity dependent pair efficiencies are estimated by an embedding technique: simulated pion pairs are embedded in real events and the reconstruction efficiency for these simulated pion pairs versus multiplicity is calculated. The pair reconstruction inefficiencies in the DC and EMCal are corrected by using pair efficiency factors estimated by the embedded MC simulation. Finally, we removed pairs within 0.005 radians in  $\Delta\phi_{DC}$  where a pair inefficiency still remains even after the correction by MC. Correction for the residual HBT effect [17] is estimated as a systematic error. The acceptance for this analysis is large, as a consequence the systematic error is  $\sim 1\%$  on each radius parameter.

In order to compare directly to previous analyses, we apply the standard “full” strength Coulomb correction calculated from the pair Coulomb wave function [6] for a 3-D Gaussian parameterization of the source using the radii obtained from the previous fit. We fit the Bose-Einstein correlation with the full Coulomb correction to the the 1-D  $q_{\text{inv}}$  parameterization,  $C_2(q_{\text{inv}}) = 1 + \lambda_{\text{inv}} \exp(-R_{\text{inv}}^2 q_{\text{inv}}^2)$ , and the 3-D Bertsch-Pratt parameterization is given by

$$C_2 = 1 + \lambda \exp(-R_{\text{side}}^2 q_{\text{side}}^2 - R_{\text{out}}^2 q_{\text{out}}^2 - R_{\text{long}}^2 q_{\text{long}}^2). \quad (1)$$

The relative momentum  $\mathbf{q}$  is decomposed into  $(q_{\text{side}}, q_{\text{out}}, q_{\text{long}})$ , where the longitudinal component ( $q_{\text{long}}$ ) is parallel to the beam axis, the out component ( $q_{\text{out}}$ ) is parallel to the mean transverse momentum of the pair,  $\mathbf{k}_T$  and the side component ( $q_{\text{side}}$ ) is perpendicular to both  $q_{\text{long}}$  and  $q_{\text{out}}$  [7, 8]. This analysis is performed in the Longitudinal Center-of-Mass System (LCMS), where the mean longitudinal momentum of the pair vanishes. In this frame, the duration of particle emission couples exclusively to  $q_{\text{out}}$ . In a general case, cross-terms may appear in Eq. 1, but they vanish in our measurement of central collisions at mid-rapidity due to symmetry reasons [18].

In the realistic source, however, many of relatively long-lived particles (e.g.  $\eta$ ,  $\eta'$ ) which decay into pions and have a Bose-Einstein interference too narrow to be resolved by experiment also have a Coulomb interaction that is negligible. For this reason, a new functional form was proposed [19] which is based upon a Core-Halo picture of the source [20] and assumes that the fraction of

pairs,  $\lambda$ , which have Bose-Einstein interference are the only pairs that contribute to the Coulomb interaction.

$$C_2 = C_{\text{core}} + C_{\text{halo}} = [\lambda(1 + G)F] + [1 - \lambda] \quad (2)$$

where  $G$  corresponds to the Gaussian term in Eq. 1, and  $F$  is the Coulomb correction term. This correction method was recently adopted by CERES [21] and STAR [22]. However, our formula differs slightly, because the momentum resolution correction to  $\lambda$  (which is small according to MC simulation) is included in our systematic error, rather than being incorporated into  $F$ .

In order to test the underlying hypothesis of Eq. 2, we fit the strength of the Coulomb interaction ( $\lambda_{+-}$ ) to the unlike-signed correlation function in the range  $0.2 < k_T < 2.0$  GeV/c, and obtained a value for  $\lambda_{+-} = 0.50 \pm 0.04$  with  $\chi^2/DoF = 3.0$ . This value is clearly inconsistent with the full strength Coulomb correction but greater than the value of  $\lambda$ , especially for  $k_T < 0.5$  GeV/c. We attribute this difference mainly to the  $\omega$  resonance, which is sufficiently long-lived to be unresolved with Bose-Einstein correlations, but may contribute significantly to the Coulomb interaction. To account for this contribution, we have modified Eq. 2 to fix the total coulomb strength at  $\lambda_{+-}$  while allowing the Bose-Einstein fraction,  $\lambda$ , to vary from zero to  $\lambda_{+-}$ ,

$$C_2 = [\lambda(1 + G)F] + [(\lambda_{+-} - \lambda)F] + [1 - \lambda_{+-}] \quad (3)$$

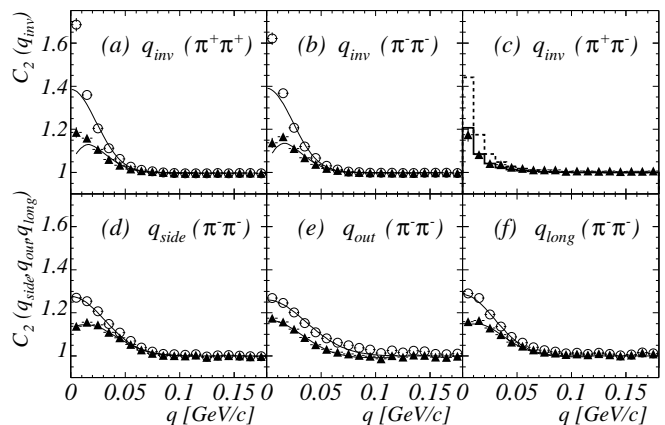


FIG. 1: Panels (a) and (b) show one-dimensional correlation functions for  $\pi^+\pi^+$  and  $\pi^-\pi^-$ . The bottom figures show the three-dimensional correlation function for  $\pi^-\pi^-$  with the full Coulomb correction (open circle) and without Coulomb (filled triangle) corrections for  $0.2 \text{ GeV}/c < k_T < 2.0 \text{ GeV}/c$  for 0-30% centrality. The projection of the 3-D correlation functions are averaged over the lowest 40 MeV in the orthogonal directions. The error bars are statistical only. The lines overlaid on the open circles (filled triangles) correspond to fits to Eq. 1 (Eq. 2) over the entire distribution. Panel (c) shows the one-dimensional correlation function of unlike-signed pions for  $0.2 < k_T < 2.0$  GeV/c. The two overlaid histograms show calculations for the full (dashed) and the 50% partial (solid) Coulomb corrections.

In applying this formula, we still calculate the additional Coulomb fraction using the Bertsch-Pratt source of approximately 5 fm, rather than estimating the larger source distribution for the  $\omega$  decay products. Therefore we use this formula to provide an upper bound on the effect of the additional Coulomb interaction. The difference between Eq. 3 and Eq. 2 is used in our estimate of the systematic errors.

Figure 1 shows the one-dimensional correlation function for  $\pi^+$  pairs,  $\pi^-$  pairs, and unlike-signed pion pairs along with projections of the three-dimensional correlation functions onto  $q_{\text{side}}$ ,  $q_{\text{out}}$  and  $q_{\text{long}}$  for  $\pi^-$  pairs.

Figure 2 shows the  $k_T$ -dependence of  $\lambda$ , Bertsch-Pratt radii, and the ratio  $R_{\text{out}}/R_{\text{side}}$  for the 30% most central events, corresponding to  $\langle N_{\text{part}} \rangle = 281$ . For the *full* Coulomb correction,  $\lambda$  is approximately constant in all the  $k_T$  bins while the radius parameters fall rapidly

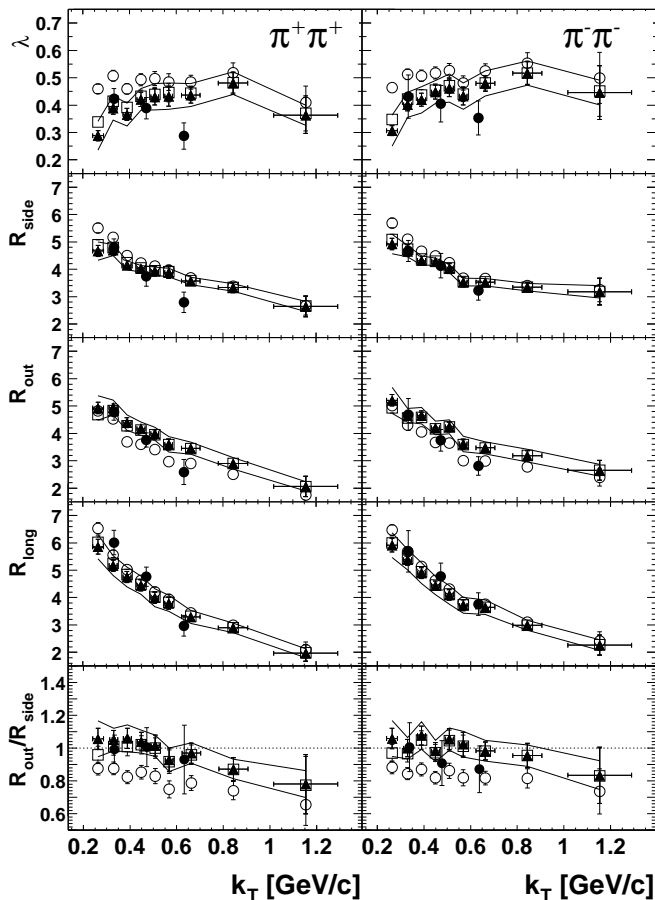


FIG. 2: The  $k_T$  dependence of the Bertsch-Pratt radius parameters and  $\lambda$  for charged pions for 0-30% centrality. Filled triangles show the results from fits to a core-halo structure by Eq. 2, with statistical error bars and systematic error bands. Open circles and squares show the results from the *full* (Eq. 1) and 50% partial (Eq. 3) Coulomb corrections with statistical error bars, respectively. Results at 130 GeV by PHENIX are given by filled circles.

with increasing  $k_T$ . The *full* Coulomb corrected radius parameters at  $\sqrt{s_{\text{NN}}} = 200$  GeV are slightly different from the *full* Coulomb corrected radius parameters at 130 GeV [12] at the same  $\langle k_T \rangle$  because of the improved pair efficiency correction, but similar within errors. For the partial Coulomb correction, results from the two different correction methods show similar trends. Compared to the *full* Coulomb correction  $R_{\text{side}}$  and  $R_{\text{long}}$  systematically decrease while  $R_{\text{out}}$  increases, and  $\lambda$  decreases in the low  $k_T$  region. In the case of the *full* Coulomb correction, the ratio  $R_{\text{out}}/R_{\text{side}}$ , in Fig. 2, is around 0.6-0.8 up to  $k_T \sim 1.2$  GeV/c. On the other hand,  $R_{\text{out}}/R_{\text{side}}$  from the partial Coulomb correction is systematically larger than that from the *full* Coulomb correction, and slightly decreases from  $\sim 1.1$  to  $\sim 0.8$  as  $k_T$  increases. Reanalysis of the 130 GeV/c data with Eq. 2 gave results that are fully consistent with the 200 GeV/c results.

Figure 3 shows the collision centrality dependence of the radius parameters. The number of participants ( $N_{\text{part}}$ ) is evaluated from the charged particle multiplicity using a Glauber model calculation [23]. To evaluate the  $N_{\text{part}}$  dependencies of the Bertsch-Pratt radius parameters

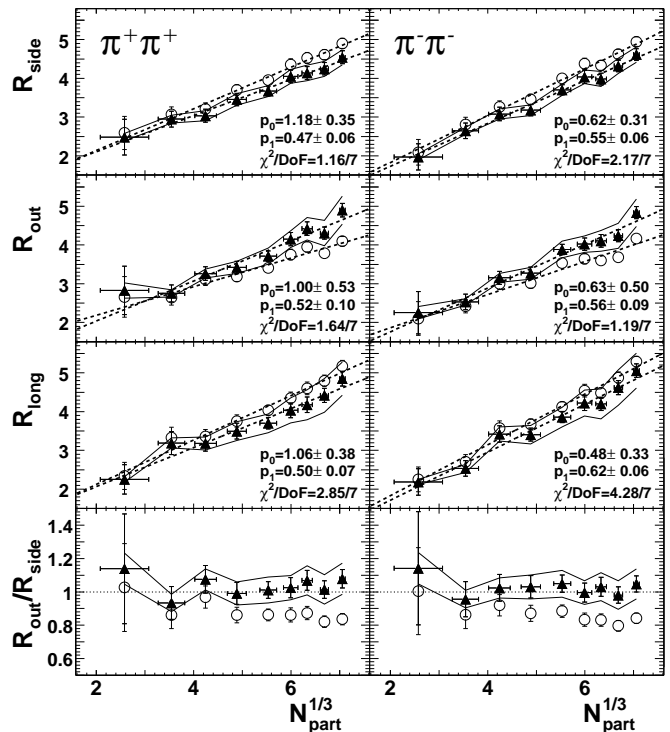


FIG. 3: Bertsch-Pratt radius parameters versus the cube root of the number of participants ( $N_{\text{part}}^{1/3}$ ) for charged pions for the fits to a core-halo structure by Eq. 2 (filled triangles) with statistical error bars and systematic error bands, in the  $0.2 \text{ GeV}/c < k_T < 2.0 \text{ GeV}/c$  range, with  $\langle k_T \rangle = 0.45 \text{ GeV}/c$ . The dashed lines show fits to  $p_0 + p_1 * N_{\text{part}}^{1/3}$ . Fitted  $p_0$  and  $p_1$  values with fits to the core-halo structure are given in each panel. The opened circles show results with the *full* Coulomb correction by Eq. 1.

ters, we fit with a function of  $p_0 + p_1 * N_{\text{part}}^{1/3}$ . For the *full* Coulomb correction, the fit  $p_1$  parameters indicate that  $R_{\text{side}}$  and  $R_{\text{long}}$  show similar  $N_{\text{part}}$  dependencies and  $R_{\text{out}}$  has a slightly smaller  $N_{\text{part}}$  dependence. For the fits to a core-halo structure, all radius parameters show similar  $N_{\text{part}}$  dependencies. All radii are consistent with a linear increase with  $N_{\text{part}}^{1/3}$ . The  $R_{\text{out}}/R_{\text{side}}$  ratios are approximately constant for all centralities. The ratios from the partial Coulomb corrections are systematically higher than those using the *full* Coulomb corrections. These fit parameters are given in Fig. 3.

In conclusion, we have presented the Bertsch-Pratt HBT radii in the LCMS for identified charged pions measured by PHENIX in Au+Au collisions at  $\sqrt{s_{\text{NN}}} = 200$  GeV. The  $k_{\text{T}}$  dependence of the HBT radii was measured for  $\langle N_{\text{part}} \rangle = 281$ , and the centrality dependence was measured for  $k_{\text{T}} = 0.45$  GeV/c. These measurements are consistent with results from Au+Au collisions at 130 GeV when a similar analysis (*full* Coulomb correction) is performed. We also performed two different partial Coulomb analyses, one based upon a self-consistent treatment of the Coulomb correction, and the other based upon direct comparison to the unlike-signed correlation, which is shown to be inconsistent with the application of a *full* Coulomb correction. Both Coulomb corrections (Eq. 2 and Eq. 3) yield similar values of  $R_{\text{out}}/R_{\text{side}}$  which slightly decreases from  $\sim 1.1$  to  $\sim 0.8$  in the range of  $k_{\text{T}} = 0.2 - 1.2$  GeV/c for  $\langle N_{\text{part}} \rangle = 281$ , and approximately constant at unity with the number of participants for  $\langle k_{\text{T}} \rangle = 0.45$  GeV/c. These detailed measurements of the transverse momentum dependence of the HBT radii, in particular that of  $R_{\text{out}}/R_{\text{side}}$ , provide extremely strong constraints for model builders.

We thank the staff of the Collider-Accelerator and Physics Departments at BNL for their vital contributions. We acknowledge support from the Department of Energy and NSF (U.S.A.), MEXT and JSPS (Japan), CNPq and FAPESP (Brazil), NSFC (China), CNRS-

IN2P3 and CEA (France), BMBF, DAAD, and AvH (Germany), OTKA (Hungary), DAE and DST (India), ISF (Israel), KRF and CHEP (Korea), RMIST, RAS, and RMAE, (Russia), VR and KAW (Sweden), U.S. CRDF for the FSU, US-Hungarian NSF-OTKA-MTA, and US-Israel BSF.

---

\* Deceased

† PHENIX Spokesperson:zajc@nevis.columbia.edu

- [1] G. Goldhaber *et al.*, Phys. Rev. **120**, (1960) 300.
- [2] U. Wiedemann, U. Heinz, Phys. Rep. **319**, (1999) 145.
- [3] T. Csörgő, Heavy Ion Phys. **15**, (2002) 1.
- [4] D.H. Rischke, M. Gyulassy, Nucl. Phys. **A597**, (1996) 701.
- [5] G.F. Bertsch, Nucl. Phys. **A498**, (1989) 173.
- [6] S. Pratt, Phys. Rev. D **33**, (1986) 72.
- [7] S. Pratt, Phys. Rev. Lett. **53**, (1984) 1219.
- [8] G. Bertsch, G.E. Brown, Phys. Rev. C **40**, (1989) 1830.
- [9] Y.M. Sinyukov, A. Makhlin, Z. Phys. C **39**, (1988) 69.
- [10] S. Pratt, T. Csörgő, J. Zimányi, Phys. Rev. C **42** (1990) 2646.
- [11] D.E. Fields *et al.*, Phys. Rev. C **52**, (1995) 986.
- [12] K. Adcox *et al.*, Phys. Rev. Lett. **88**, (2002) 192302.
- [13] C. Adler *et al.*, Phys. Rev. Lett. **87**, (2001) 082301.
- [14] M. Gyulassy, nucl-th/0106072, Lect. Notes Phys. **583**, (2002) 37-79.
- [15] K. Adcox *et al.*, Nucl. Instrum. Methods **A499**, (2003) 469.
- [16] GEANT 3.2.1, CERN program library.
- [17] W.A. Zajc *et al.*, Phys. Rev. C **29**, (1984) 2173.
- [18] S. Chapman, P. Scotto, U. Heinz, Phys. Rev. Lett. **74**, (1995) 4400; Heavy Ion Phys. **1**, (1995) 1.
- [19] Y.M. Sinyukov, R. Lednicky, S.V. Akkelin, J. Pluta, B. Erazmus, Phys. Lett. B **432**, (1998) 248.
- [20] T. Csörgő *et al.*, Eur. Phys. J. C **9**, (1999) 275.
- [21] D. Adamova *et al.*, nucl-ex/0207005.
- [22] J. Adams *et al.*, nucl-ex/0312009.
- [23] K. Adcox *et al.*, Phys. Rev. Lett. **86**, (2001) 3500.